Apical Polarity of N-CAM and EMMPRIN in Retinal Pigment Epithelium Resulting from Suppression of Basolateral Signal Recognition

Alan D. Marmorstein,* Yunbo C. Gan,* Vera L. Bonilha,* Silvia C. Finnemann,* Karl G. Csaky,‡ and Enrique Rodriguez-Boulan*

*Margaret M. Dyson Vision Research Institute, Department of Ophthalmology and Department of Cell Biology and Anatomy, Cornell University Medical College, New York 10021; and ‡Laboratory of Immunology, National Eye Institute, Bethesda, Maryland 20892

Abstract. Retinal pigment epithelial (RPE) cells apically polarize proteins that are basolateral in other epithelia. This reversal may be generated by the association of RPE with photoreceptors and the interphotoreceptor matrix, postnatal expansion of the RPE apical surface, and/or changes in RPE sorting machinery. We compared two proteins exhibiting reversed, apical polarities in RPE cells, neural cell adhesion molecule (N-CAM; 140-kD isoform) and extracellular matrix metalloproteinase inducer (EMMPRIN), with the cognate apical marker, p75-neurotrophin receptor (p75-NTR). N-CAM and p75-NTR were apically localized from birth to adulthood, contrasting with a basolateral to apical switch of EMMPRIN in developing postnatal rat RPE. Morphometric analysis demonstrated that this switch cannot be attributed to expansion of the apical surface of maturing RPE because the basolateral membrane expanded proportionally, maintaining a 3:1 apical/basolateral ratio. Kinetic analysis of polarized surface delivery in MDCK and RPE-J cells showed that EMMPRIN has a basolateral signal in its cytoplasmic tail recognized by both cell lines. In contrast, the basolateral signal of N-CAM is recognized by MDCK cells but not RPE-J cells. Deletion of N-CAM's basolateral signal did not prevent its apical localization in vivo. The data demonstrate that the apical polarity of EMMPRIN and N-CAM in mature RPE results from suppressed decoding of specific basolateral signals resulting in randomized delivery to the cell surface.

Key words: adenovirus gene transfer • interphotoreceptor matrix • p75-NTR • polarity • RET-PE2

THE retinal pigment epithelium (RPE)[1] is a highly specialized derivative of the embryonic neural tube that lies with its apical surface in intimate contact with the light-sensitive cells of the retina (Zinn and Marmor, 1979), performing critical transport, barrier, and phagocytic support functions for the neural retina. These functions of RPE cells require a characteristic apical distribution of certain proteins that are usually found on the basolateral membrane in other epithelia. For example, apical Na,K-ATPase provides a high Na$^+$ environment appropriate for photoreceptor function (Bok, 1982; Okami et al., 1990; Gundersen et al., 1991; Gallemore et al., 1997; Miller and Steinberg, 1977; Rizzolo, 1997; Zhao et al., 1997). The apical localization of the neural cell adhesion molecule N-CAM-140 in RPE (Gundersen et al., 1993), which overrides a dominant basolateral signal in the cytoplasmic domain recognized by MDCK cells (Powell et al., 1991; Le Gall et al., 1997), is presumably required to regulate adhesive contacts with photoreceptors and the interphotoreceptor matrix (IPM), an extracellular substance produced by both RPE and photoreceptors (Tawara et al., 1989; Landers et al., 1991). The immunoglobulin superfamily member EMMPRIN (extracellular matrix metalloproteinase inducer; also known as RET-PE2 antigen, basigin, M6, and CE-9; Finnemann et al., 1997a) is basolaterally polarized in rat hepatocytes (Bartles et al., 1985a,b), kidney, and other epithelia (Finnemann et al., 1997a) but is apical in mature RPE (Marmorstein et al., 1996). Since EMMPRIN stimulates the production of matrix metalloproteinases (MMPs) in fibroblasts (Biswas et al., 1995; Guo

1. *Abbreviations used in this paper*: DAPI, 4′,6-diamidino-2-phenylindole; EMMPRIN, extracellular matrix metalloproteinase inducer; IPM, interphotoreceptor matrix; MMP, matrix metalloproteinase; N-CAM, neural cell adhesion molecule; p75-NTR, p75-neurotrophin receptor; RPE, retinal pigment epithelium.

et al., 1997), and MMPs 1, 2, 3, and 9 have been found in the IPM (Plantner et al., 1998), probably secreted apically by RPE (Padgett et al., 1997), EMMPRIN's switch to the apical surface may play a key role in the remodelling and maintenance of IPM. While the functional requirements for the apical polarity of certain proteins in RPE cells can be rationalized, the mechanisms involved in their polarity shift are completely unknown.

A major difference between RPE cells and other simple epithelia is that the apical surface is not free but makes direct contact with the IPM and photoreceptor outer segments (Johnson et al., 1986). This interaction is likely to play a fundamental role in the reversed polarity of selected plasma membrane proteins (Rizzolo, 1990; Gundersen et al., 1991, 1993; Rizzolo and Heiges, 1991; Rizzolo et al., 1994, Rizzolo and Zhou, 1995; Marmorstein et al., 1996). An excellent model to study the role of photoreceptor/RPE/IPM interactions in RPE polarity is the developing retina of the newborn rat. Mature interactions between RPE and photoreceptors do not exist in the newborn rat: the photoreceptors lack outer segments, the apical microvilli of RPE cells are short with respect to those of the adult, and the IPM has not been yet produced. However, by postnatal day 12 (P12), the characteristic structural and functional features of the adult retina are established: microvilli on the apical surface of RPE cells form sheaths surrounding photoreceptor outer segments, and IPM (Dowling and Gibbons, 1962; Olney, 1968; Braekevelt and Hollenberg, 1970) and phagocytosis of outer segments is turned on (Ratto et al., 1991). The elongation of microvilli results in a net increase in the apical surface area during the first 2 wk of life (Rizzolo, 1997; Zhao et al., 1997). It is unclear whether the apical polarization of N-CAM (Gundersen et al., 1993) or EMMPRIN (Marmorstein et al., 1996) is passively accounted for by this enlargement of the apical membrane or is the result of specific changes in the cellular sorting machinery triggered by the developing interactions with the IPM and photoreceptors.

In this paper, we took advantage of in vivo gene transfer technology to express genes encoding mutant plasma membrane proteins into RPE in vivo. Our goal was to identify a mechanism to account for the reversed apical polarity of EMMPRIN and N-CAM in RPE cells. To this end, we studied the relative contributions of changes in cell shape and intracellular protein sorting during rat retinal postnatal development to the apical polarization of these proteins. We investigated the relative distributions in developing rat retina of N-CAM, EMMPRIN, and human p75-neurotrophin receptor (p75-NTR), a well-characterized apical marker with a defined apical signal in MDCK cells (Le Bivic et al., 1991; Monlazeur et al., 1995; Yeaman et al., 1997), and studied morphometrically the maturing RPE at the time it develops contacts with the neural retina. To obtain information on the ability of RPE to recognize basolateral sorting signals defined originally in MDCK cells, we (*a*) compared the intracellular targeting pathways of EMMPRIN and N-CAM in MDCK cells and in the model RPE cell line RPE-J, and (*b*) studied the polarity of N-CAM devoid of its basolateral signal introduced into RPE in vivo via subretinal injection of adenovirus vectors. Our results suggest that mature RPE cells possess the ability to regulate the entry of specific basolat-eral proteins into the basolateral pathway by selectively turning off basolateral signal decoding mechanisms.

Materials and Methods

Cell Culture

All cell culture reagents were purchased from Life Technologies (Gaithersburg, MD) unless otherwise indicated. RPE-J cells were maintained at 32°C in a 95% air/5% CO_2 atmosphere in DME containing 4% CEL-LECT Gold fetal bovine serum (ICN Pharmaceuticals, Costa Mesa, CA), nonessential amino acids, penicillin/streptomycin, and glutamine as described previously (Nabi et al., 1993; Marmorstein et al., 1996). For all studies, RPE-J cells were plated at a density of 350,000 cells/cm^2 on 1.2-cm-diameter Transwell filters (Corning Inc., Corning, NY) coated with Matrigel (Collaborative Research, Bedford, MA). Cells were grown for 6–7 d at 32°C and then transferred to 39.5°C for 36–42 h before use.

MDCK cells were maintained in DME containing 10% FBS, glutamine, and penicillin/streptomycin at 37°C in a 95% air/5% CO_2 atmosphere. For all experiments, cells were plated 5 d before use on 2.4-cm-diameter Transwell filters at a density of 250,000 cells/cm^2.

The transformed human kidney cell line 293 (American Type Culture Collection, Rockville, MD) was maintained as a monolayer in Improved Eagle's Minimum Essential Medium (Biofluids Inc., Rockville, MD), supplemented with L-glutamine at 10 mM, penicillin G at 50 U/ml, streptomycin at 50 µg/ml, and 10% heat-inactivated fetal bovine serum (Hyclone Laboratories, Logan, UT) in a 5% CO_2 humidified air incubator at 37°C. Transfections and transductions of 293 cells were performed generally at 60–80% confluence.

EMMPRIN Plasmids and Transfections

All of the constructs used in this study are indicated in Fig. 1. The cloning of the RET-PE2/EMMPRIN DNA into the mammalian expression vector pBk has been described elsewhere (Finnemann et al., 1997a). In this manuscript, the plasmid is referred to as pBk-EMMPRIN. The EMMPRIN truncation mutants, 244t and 203t (corresponding to the COOH-terminal amino acid counted from the initiation methionine of rat EMMPRIN), were constructed using PCR amplification using pBk-EMMPRIN as template. T3 primer (Operon Technologies, Inc., Alameda, CA) was used as the 5′ primer in both reactions. Unique 3′ primers inserted a stop codon and ApaI restriction site at the site of truncation. The sequence of the 3′ primers was as follows: 203t, CCCGGGCCCTCACACACG-CAGTGAGATGG; 244t, CCCGGGCCCCCTCGTAGATGAAGATGA. PCR products were gel purified, digested with EcoRI and ApaI, and subcloned into pCDNA3 or pBk. Fusion of p75-NTR and the N-CAM basolateral sorting signal in the plasmid pCB7 is described elsewhere (Le Gall et al., 1997).

MDCK or RPE-J cells plated on 10-cm^2 plates were transfected using the calcium phosphate procedure (Graham and Van der Eb, 1973) and selected with 500 µg/ml G418. 10 d into the selection, foci were isolated by ring cloning, and their expression was checked by immunofluorescence and/or Western blotting. The level of expression and number of cells expressing EMMPRIN or EMMPRIN mutants varied amongst clones but remained constant during serial passage.

Preparation of Replication-defective Adenovirus Vectors

Ad5CMVp75, a type 5 replication-defective adenovirus encoding p75-NTR (Yoon et al., 1996), was obtained from Dr. Moses Chao (Cornell University Medical College). Ad-NCAM749t, a type 5 replication-defective adenovirus encoding a truncated form of chicken N-CAM lacking a basolateral sorting signal in its cytoplasmic domain (NCAM749t [Le Gall et al., 1997]) was produced as follows. NCAM749t cDNA was subcloned from the plasmid pCMV5-NCAM749t (Le Gall et al., 1997) into the XbaI and ClaI sites of the adenovirus shuttle plasmid pAdeno-1 (Sullivan et al., 1996). 10 µg of the resultant plasmid (pAdeno-NCAM-749t) was cotransfected along with 5 µg of the adenovirus type 5 genome containing plasmid pJM17 (provided by Dr. Frank L. Graham, McMaster University, Hamilton, Ontario, Canada) by calcium phosphate coprecipitation (Wigler et al., 1977) into 293 cells. Single plaques of Ad-NCAM749t were isolated and amplified in 293 cells. All virus stocks used for these studies were amplified from single plaques and purified from crude viral lysates
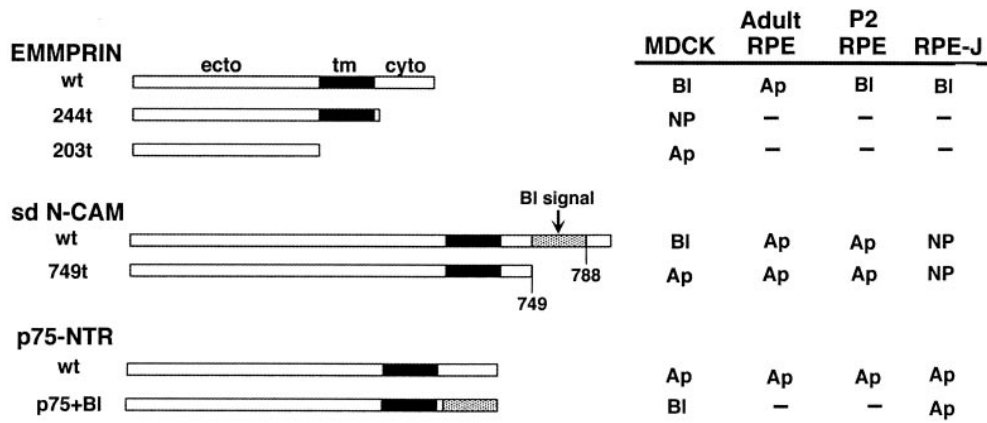
Figure 1. Mutants constructed to characterize basolateral targeting information in EMMPRIN and N-CAM. A cytoplasmic deletion (EMMPRIN-244t) and a secreted form of EMMPRIN (EMMPRIN-203t) were generated as described in Materials and Methods to determine if basolateral sorting information exists in the EMMPRIN molecule. The N-CAM749t mutant represents a form of N-CAM that is lacking a basolateral targeting signal and was incorporated into an E1-deleted replication-defective adenovirus as described in Materials and Methods. p75 + Bl is a fusion of p75 with the 40–amino acid basolateral targeting signal from N-CAM. Both N-CAM749t and p75 + Bl were constructed as described in Le Gall et al. (1997). The table at the right summarizes the steady-state polarities of the different constructs in various cell lines and in RPE cells in vivo.

on a discontinuous cesium chloride gradient as described elsewhere (Spector et al., 1997).

Transduction of RPE-J Cells with Replication-defective Adenoviruses

RPE-J cells grown on Transwell filters for 6–7 d at 32°C were washed once with infection medium (DME containing 20 mM Hepes and 0.2% bovine serum albumin). After removal of apical and basolateral medium, 100 μl of infection medium containing either Ad5CMVp75 or Ad-NCAM79t at an MOI of 1–3 (~20–80 particles/cell) was placed in the apical compartment. The cells were incubated at 32°C. After 2 h, medium was added back to both the apical and basolateral compartments, and the cells were switched to a 39.5°C incubator. All assays were conducted on cells 36–42 h after transduction.

Domain-specific Biotinylation Assay for Steady-State Polarity and Protein Targeting Assay

Domain-selective biotinylation for steady-state polarity and biotin targeting assays were performed as described elsewhere (Marmorstein et al., 1996, 1998) using either alkaline phosphatase–conjugated streptavidin (Sigma Chemical Co., St. Louis, MO) and enhanced chemifluorescence detection (see below, SDS-PAGE and Western blotting), or ^{125}I-streptavidin and a phosphorimager (model STORM 860; Molecular Dynamics, Sunnyvale, CA) for steady-state assays. For targeting assays ^{35}S-labeled proteins were detected using uncoated phosphorscreens and read on the STORM 860 phosphorimager. Data were quantified using Imagequant version 1.2 (Molecular Dynamics).

SDS-PAGE and Western Blotting

SDS-PAGE was performed according to the method of Laemmli (1970). Gels were transferred to polyvinyl difluoride membranes, and blots were performed as previously described (Finnemann et al., 1997a) with the following modification. Secondary antibodies were conjugated to alkaline phosphatase, and blots were visualized using the Vistra enhanced chemifluorescence kit (Amersham Corp., Arlington Heights, IL) in conjunction with a STORM 860 phosphorimager according to the manufacturer's instructions.

Immunofluorescence and Confocal Microscopy

Eyecups or RPE-J monolayers were fixed for 30 min in 4% paraformaldehyde in PBS containing 1.3 mM CaCl$_2$, 1.0 mM MgCl$_2$ (PBS/CM) and quenched with 50 mM NH$_4$Cl in PBS/CM. For cryosectioning, eyecups were infiltrated with 30% sucrose in PBS/CM and then with OCT (Tissue Tek®; Miles Inc., Elkhart, IN). When it was desirable to maintain the RPE–neural retina interaction, rats were killed by CO$_2$ asphyxiation and subjected to intracardiac perfusion with HBSS followed by 4% paraformaldehyde in PBS/CM. Perfusion-fixed eyes were enucleated, the corneas were incised, and then further immersion fixed overnight. Monolayers or sections were stained with a rabbit polyclonal antisera raised against rat laminin (GIBCO BRL), rat EMMPRIN (obtained from J. Bartles, Northwestern University, Chicago, IL), or N-CAM (obtained from B. Cunningham) and/or mouse monoclonal antibodies RET-PE2 (against rat EMMPRIN, provided by Dr. James Neill, SUNY Health Science Center at Brooklyn, Brooklyn, NY), Me20.4 (recognizing p75-NTR), or 5e (recognizing chicken N-CAM) and then with appropriate CY3 or FITC-conjugated secondary antibodies (Jackson ImmunoResearch, West Grove, PA). The cells were washed, and nuclei were stained either with propidium iodide or 4',6-diamidino-2-phenylindole (DAPI). Filters were excised and mounted in Vectashield (Vector Labs, Burlingame, CA). Whole eyecup preparations were cut radially and mounted en face. Labeled cells were visualized with an epifluorescence microscope (model Axiovert 35; Carl Zeiss, Inc., Thornwood, NY), a microscope (model E600, Nikon, Inc., Melville, NY) equipped with a cooled CCD camera, or a dual channel laser scanning confocal microscope (Sarastro/Molecular Dynamics, Sunnyvale, CA) as previously described (Hanzel et al., 1991). Images were photographed on Kodak Ektachrome film and scanned, or digitally acquired images were translated using Metamorph (Universal Imaging) or NIH Image 1.52 software. All images were recompiled in Adobe Photoshop 4.0 (San Jose, CA).

Electron Microscopy and Morphometry

The position of tight junctions was assessed using ruthenium red on differentiated monolayers of RPE-J cells as previously described (Nabi et al., 1993). To assess the effect of subretinal injection on the RPE–neural retina interface, rats injected subretinally as described below were perfused intracardially with 2.5% glutaraldehyde in PBS/CM. After enucleation, the anterior segments of eyes were removed above the ora serrata. Neural retina–free eyecups were prepared as described above and fixed by immersion overnight in 0.1 M sodium cacodylate buffer containing 2.5% glutaraldehyde, 4% paraformaldehyde, and 10% saturated picric acid. After dehydration, en bloc staining with uranyl acetate, and embedding in Epon, 60–70-nm sections were cut using a diamond knife (Diatome, U.S., Fort Washington, PA). Sections were stained with lead citrate and examined at 80 kV in an electron microscope (model JEOL-100 CXII; JEOL U.S.A., Peabody, MA). Morphometry was performed essentially as described (Okami et al., 1990; Butor and Davoust, 1992) with the following modifications. Apical and basolateral membrane lengths were determined from electron micrographs of RPE-J monolayers, P2, and adult RPE photographed at 4,800 and 14,000×. Negatives were scanned, and apical and basolateral membranes were traced in black using a graphic digitizing tablet, Adobe Photoshop 3.0, and an Apple Macintosh 9500 computer. To avoid counting intracellular membranes as basolateral, basolateral folds/tubules were traced only when there was a clear path to the basal surface.

The number of black pixels in each tracing was determined using NIH Image 1.52 and converted into micrometers by normalizing to pixel density and magnification.

Subretinal Injection

All animal procedures were in accordance with institutional guidelines. Approximately 60 adult Long-Evans rats and 14 litters (average 10–12 pups/litter) were used in this study. Adult rats were injected in one eye subretinally with 15–20 μl of HBSS or HBSS containing ∼10^7 pfu/μl of Ad5CMVp75 or Ad-NCAM749t as previously described (Bonilha, 1997). After injection, the animal was allowed to recover for a period of 5–7 d.

Newborn (P0) and P7 pups were injected subretinally using a *trans*-scleral approach. Pups were anesthetized by cold-induced hypothermia. Under an ophthalmic microscope the eyelid of one eye was opened. A single incision penetrating to the vitreous was made to provide pressure relief on the nasal side of the eye close to the limbus. A 30-gauge needle was then inserted into the subretinal space through the sclera opposite the incision. With the needle in place, 3–5 μl of HBSS or HBSS containing ∼10^7 pfu/μl of Ad5CMVp75 or Ad-NCAM749t was injected. The needle was slowly withdrawn and the eyelid closed with 7-0 surgical silk. Pups were allowed to recover from hypothermia and were then returned to the dam.

Results

Localization of p75-NTR, EMMPRIN, and N-CAM in Maturing and Adult RPE

The first set of experiments was designed to compare by immunofluorescence microscopy in developing rat RPE the relative polarities of N-CAM, and EMMPRIN, cognate basolateral markers in other epithelia, with that of p75-NTR, a cognate apical marker of other epithelia. Previous work has shown that N-CAM is apically polarized in adult RPE and EMMPRIN switches to the apical surface during the first postnatal week in the rat (Gundersen et al., 1993; Marmorstein et al., 1996). Human p75-NTR was introduced into RPE at P0 and at the adult stage by adenovirus-mediated gene transfer. Since subretinal injection of adenoviruses (between RPE and photoreceptors) causes detachment of the neural retina, we carried out controls to establish that the two layers had reattached.

Transduction of P75-NTR into Adult RPE Cells In Vivo. Codistribution with EMMPRIN at the Apical Surface. We injected the Ad5CMVp75 vector into the subretinal space of adult male and female Long-Evans rats. Histological analysis of injected eyes fixed by intracardiac perfusion with 2.5% glutaraldehyde indicated that the RPE–neural retina interaction was reestablished within 48 h of the surgery (Fig. 2 *A*). Electron microscopic examination (data not shown) revealed longitudinal microvilli penetrating the space between photoreceptor outer segments, with only sparse areas showing transverse microvilli flattened against the apical surface of RPE, and recently phagocytosed ROS, indicative of a functional interaction between RPE cells and the neural retina. p75-NTR expression was detected by immunoprecipitation and streptavidin blot of surface biotinylated RPE from eyes enucleated 5 d after injection. A cluster of bands was detected in the 50–80-kD range in Ad5CMVp5-infected cells but not in sham-injected controls (data not shown), with some widening of the bands likely due to proteolysis during sample preparation. Thus, RPE cells transduced in vivo with adenoviruses carrying p75-NTR efficiently expressed this protein, and the RPE–neural retina interface was faithfully restored.

Immunofluorescence staining of whole mounted neural retina–free eyecups detected p75-NTR on the apical microvilli of adult RPE (Fig. 2 *B*). Double immunofluorescence of cryosections of the same eyes with laminin antibodies (Fig. 2 *C*) detected a clear separation between apical p75-NTR, at the interface with the neurosensory retina, and laminin staining at the RPE's basement membrane (Fig. 2, *C* and *D*, *Bm*), at the interface with the choroid (*Ch*). A perfect colocalization of EMMPRIN and p75-NTR was detected in cryosections of neural retina–free eyecups prepared from adult eyes (Fig. 2, *I–K*, *Adult*).

p75-NTR and EMMPRIN Polarize to Opposite Surfaces in Immature RPE. If the apical polarity of N-CAM and/or EMMPRIN depends on the interaction of the apical membrane of RPE with the neural retina and the IPM, it might be different in the immature RPE of newborn rats, when neither the IPM nor the photoreceptor outer segments have yet developed. To test this hypothesis, we compared the respective localization of p75-NTR and EMMPRIN in the immature retina of newborn rats. Newborn (P0) Long-Evans rats were injected in the subretinal space with the Ad5CMVp75 vector in HBSS or with HBSS alone. At various times thereafter, animals were killed, and the polarities of p75-NTR and EMMPRIN were determined by double immunofluorescence microscopy. At the earliest time point examined, P2, p75-NTR was present on the apical surface (Fig. 2 *E*), whereas EMMPRIN was predominantly basolateral or nonpolar (Fig. 2 *F*). Overlap of the two images indicated that, while there was some colocalization of the two proteins at the apical surface, their distributions were clearly different (Fig. 2 *G*). Accordingly, EMMPRIN adopted a honeycomb pattern, whereas p75-NTR localized on the short microvilli in immature RPE at P2 (data not shown).

N-CAM Is Apically Polarized in Newborn and Adult RPE Cells. As previously reported (Gundersen et al., 1993), N-CAM was found to be apically polarized in adult RPE cells (Fig. 2 *L*). However, in stark contrast with EMMPRIN, endogenous N-CAM was also found to be apically polarized at P2 (Fig. 2 *H*). Thus, while adult RPE cells lack the ability to segregate the basolateral markers N-CAM and EMMPRIN from p75-NTR, immature RPE cells express it selectively, by sorting EMMPRIN, but not N-CAM, to the basolateral surface. In immature RPE, both N-CAM and p75-NTR are localized apically, as in adult RPE.

Immature and Mature RPE Have Identical Apical/Basolateral Surface Area Ratios. We hypothesized that the expansion of the apical surface might be an important contributor to EMMPRIN's polarity switch while enhancing the apical polarization of N-CAM. To test this hypothesis, we performed a morphometric analysis of the ratio of apical and basolateral membranes in P2 and adult RPE cells to determine the potential contribution of cell shape to the changes in polarity described above. For consistency between our immunofluorescence and morphometric analyses, we used neural retina–free preparations of P2 and adult RPE. Fig. 3, *A* and *B*, shows that not only do the apical microvilli expand during the first two postnatal weeks, but the basal surface, represented by an intricate network of folds and tubular extensions of the basal plasma membrane that contact with the basement membrane (Fig. 3, *arrows*), also expands. In contrast to adult RPE cells,
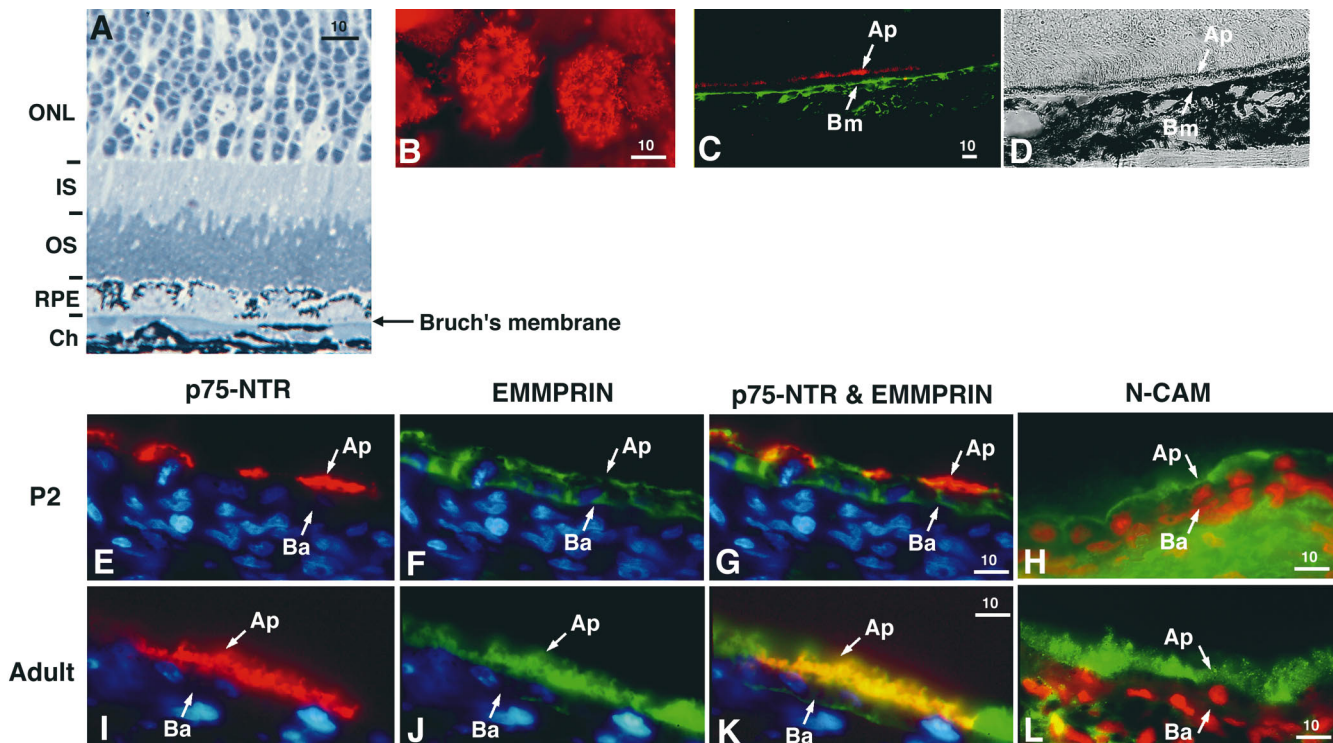
Figure 2. Steady-state polarity of EMMPRIN, p75-NTR, and N-CAM in RPE cells. p75-NTR was expressed in P0 or adult RPE cells in vivo via adenovirus-mediated gene transfer. Animals injected at P0 were killed at P2 (*E–H*), and adults were killed 5 d after injection. Eyes were fixed with 2.5% glutaraldehyde (*A*) or 4% paraformaldehyde either by intracardiac perfusion (*A*, *C*, and *D*) or by immersion in 4% paraformaldehyde after removal of the neural retina (*B* and *E–L*). *A* is a 1-μm-thick section of an eye 5 d after subretinal injection with AdCMVp75 stained with methylene blue. Note that the retina has fully reattached and is making intimate contact with the apical surface of the RPE cells. The photoreceptor layer appears unaffected by the injection since the number of photoreceptor nuclei in the outer nuclear layer (*ONL*) appears undiminished. One effect of the injection is the minor vacuolation of the inner (*IS*) and outer (*OS*) segments. p75-NTR staining in whole mounts of adult (*B*) eyes was above the plane of pigment granules, which would otherwise interfere with the fluorescence signal and was clearly associated with apical microvilli. The apical polarity of p75-NTR is confirmed in 10-μm cryosections (*C*, *E*, *G*, *I*, and *K*), prepared, and stained for p75-NTR (*red*) and laminin (*green* in *C*), or p75-NTR and EMMPRIN (*green* in *F*, *G*, *J*, and *K*). p75-NTR staining was confined to RPE cells (see bright field, *D*) and was clearly apical to and distinct from laminin staining, which labels Bruch's membrane (*Bm*). In neural retina–free sections of adult eyes, p75-NTR (*red* in *E* and *G*), like EMMPRIN (*green* in *E* and *G*) in the same section, was present on the apical surface of the cells as demonstrated by their colocalization in *K*. At P2, however, p75-NTR was apical (*E* and *G*), but EMMPRIN was nonpolar or basolateral at P2 (*F* and *G*). In uninjected eyes, N-CAM (*green* in *H* and *L*) was apically polarized in RPE cells both at P2 and in adults. Nuclei were stained blue by DAPI, except in *H* and *L*, where they appear red and were stained with propidium iodide. *Ap*, apical; *Ba*, basal; *Ch*, choroid. Bars, 10 μm.

which exhibited elongated microvilli and intense basolateral folding (Fig. 3 *B*), P2 RPE cells had short microvilli and few basolateral folds (Fig. 3 *A*). Interestingly, the ratio of apical/basolateral membrane did not significantly change from P2 to adulthood and remained near 3:1 (Table I) because of the doubling of both apical and basolateral surface areas during postnatal development. These results suggest that basolateral sorting of EMMPRIN at P2 is an active process since uniform distribution of the protein in the plasma membrane of these highly asymmetric cells would result in an apparent apical polarity. Indeed, since the basolateral surface accounts for only 27% of the total plasma membrane at P2, the concentration of EMMPRIN in the basolateral plasma membrane at this time must require some form of post-Golgi basolateral sorting.

Surface Localization and Targeting of p75-NTR, EMMPRIN, and N-CAM in RPE-J Cells

To gain information on the routes followed by these pro-teins to the surface of RPE cells, we performed targeting assays in the RPE-J cell line, which can be grown on Transwell filters. Previous work has shown that these cells generate transepithelial monolayer resistances of over 200 $\Omega \cdot cm^2$. Morphometric analysis of these cells was performed considering that the tight junctions are localized midway through the lateral membrane, as indicated by the presence of a barrier to diffusion of the electron-dense tracer ruthenium red (Fig. 3 *C*) added to the apical surface. RPE-J cells grown on polycarbonate filters were found to have nearly equal amounts of apical and basolateral membranes (Table I), which is similar to MDCK cells grown on polycarbonate filters (Butor and Davoust, 1992).

Steady-State Polarity of P75-NTR and N-CAM in RPE-J Cells. The p75-NTR cDNA was expressed by transduction with Ad5CMVp75, and the polarity of the protein was analyzed after 48 h. As observed by confocal microscopy, p75-NTR localized predominantly to the apical domain of RPE-J cells (Fig. 4 *A*), as in native RPE (Fig. 2). Domain-specific biotinylation demonstrated that p75-NTR is 78 ±
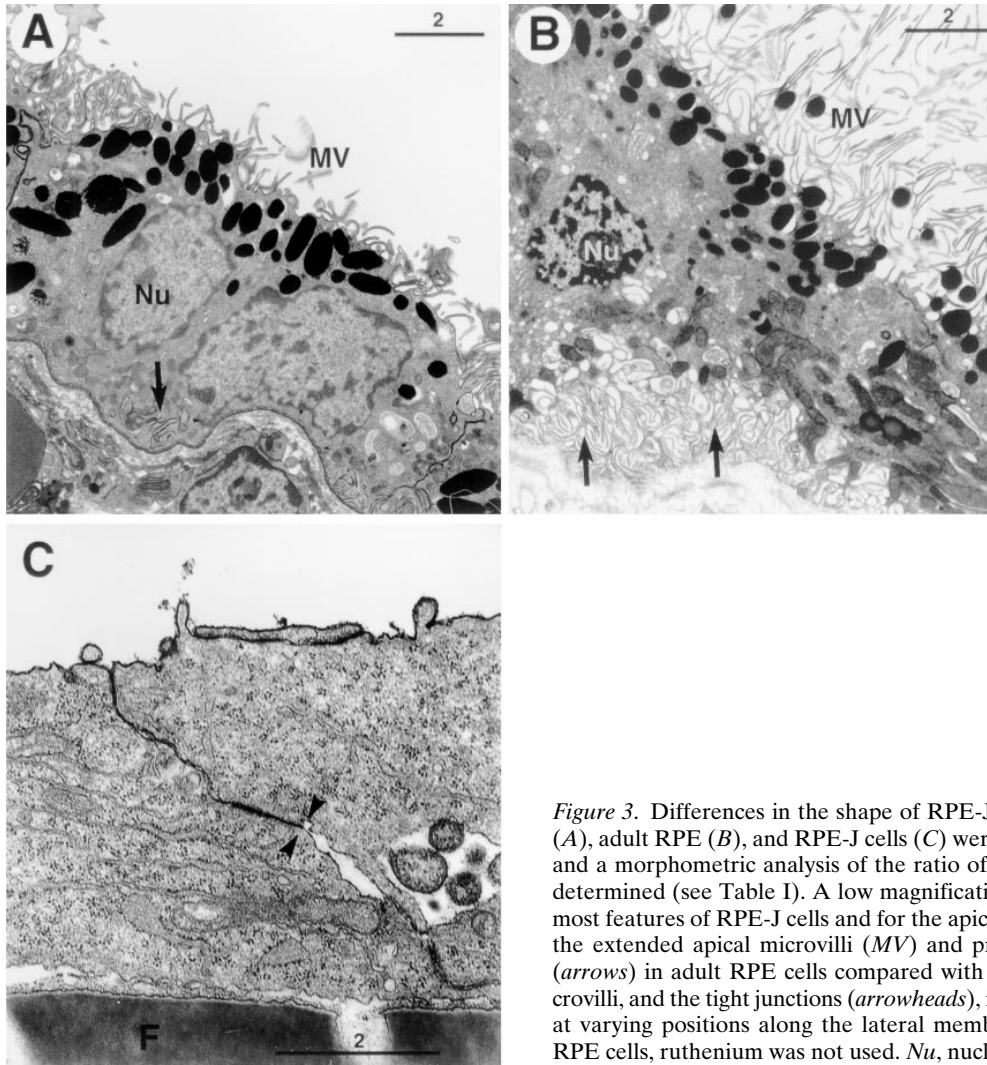
Figure 3. Differences in the shape of RPE-J, P2 RPE, and adult RPE cells. P2 (*A*), adult RPE (*B*), and RPE-J cells (*C*) were examined by electron microscopy and a morphometric analysis of the ratio of apical and basolateral membranes determined (see Table I). A low magnification (4,800) was sufficient to discern most features of RPE-J cells and for the apical surface of RPE cells in situ. Note the extended apical microvilli (*MV*) and prominence of the basolateral folds (*arrows*) in adult RPE cells compared with P2 cells. RPE-J cells have few microvilli, and the tight junctions (*arrowheads*), identified using ruthenium red, were at varying positions along the lateral membrane of the cells. In P2 and adult RPE cells, ruthenium was not used. *Nu*, nucleus, *F*, Transwell filter. Bars, 2 μm.

10% ($n = 6$) apical in RPE-J cells (Fig. 4 *B*), a value similar to that reported in MDCK cells transduced with Ad5CMVp75 (Yeaman et al., 1997).

We have previously reported that N-CAM assumes a lateral localization in RPE-J cells (Nabi et al., 1993). This result was confirmed using confocal microscopy (Fig. 4 *C*). However, domain-specific biotinylation assays (Fig. 4 *D*) consistently indicated that N-CAM was distributed nonpolarly at the cell surface. This apparent paradox is solved if one considers the presence of the tight junction midway through the lateral surface of RPE-J cells, as indicated above (Fig. 3 *C*), and the results of the morphometric analysis of RPE-J cells that demonstrate equal amounts of membrane above and below the level of the tight junction in these cells. The lateral localization of N-CAM might be attributed to lateral "trapping" by homotypic contacts with N-CAM molecules in neighboring cells or by heterotypic interactions with extracellular matrix components.

Vectorial Targeting of p75-NTR in RPE-J Cells. Analysis of total immunoprecipitates from cell lysates obtained at different chase times showed that p75-NTR was processed from the precursor ~60-kD form to the *O*-glycanated/*N*-glycanated 75-kD Golgi form at ~1–2 h of chase

(Fig. 5, *A–C*). The appearance of p75-NTR at the RPE-J cell surface occurred very shortly after Golgi processing, at ~1 h, and reached steady-state levels after ~2 h, indicating that the transport time between Golgi and the cell surface was very short. Most of p75-NTR appeared predominantly at the apical cell surface, at similar proportions (~80% apical) as observed at steady state (Fig. 5 *C*). Thus, both steady-state distribution and surface delivery of p75-NTR in RPE-J are identical to those previously reported in MDCK cells. Unlike MDCK cells, however, the half-life of p75-NTR at the cell surface of RPE-J cells was long (22 h vs. ~2 h in MDCK cells) (Le Bivic et al., 1991, Yeaman, 1997). These results demonstrate for the first time that a direct pathway to the apical surface exists in RPE cells. As

Table I. Apical and Basolateral Membrane Lengths

Cell	Mean ± SD Apical	Mean ± SD Basolateral	Apical/ Basolateral	Percent apical membrane	n
	μm	μm			
Adult RPE	284 ± 50	104 ± 23	2.7:1	73	23
P2 RPE	132 ± 40	51 ± 21	2.6:1	72	27
RPE-J	40 ± 30	34 ± 22	1.2:1	55	23

A

X-Y

X-Z

B

kD	Ap	Bl
97.4		
69		
46		

D

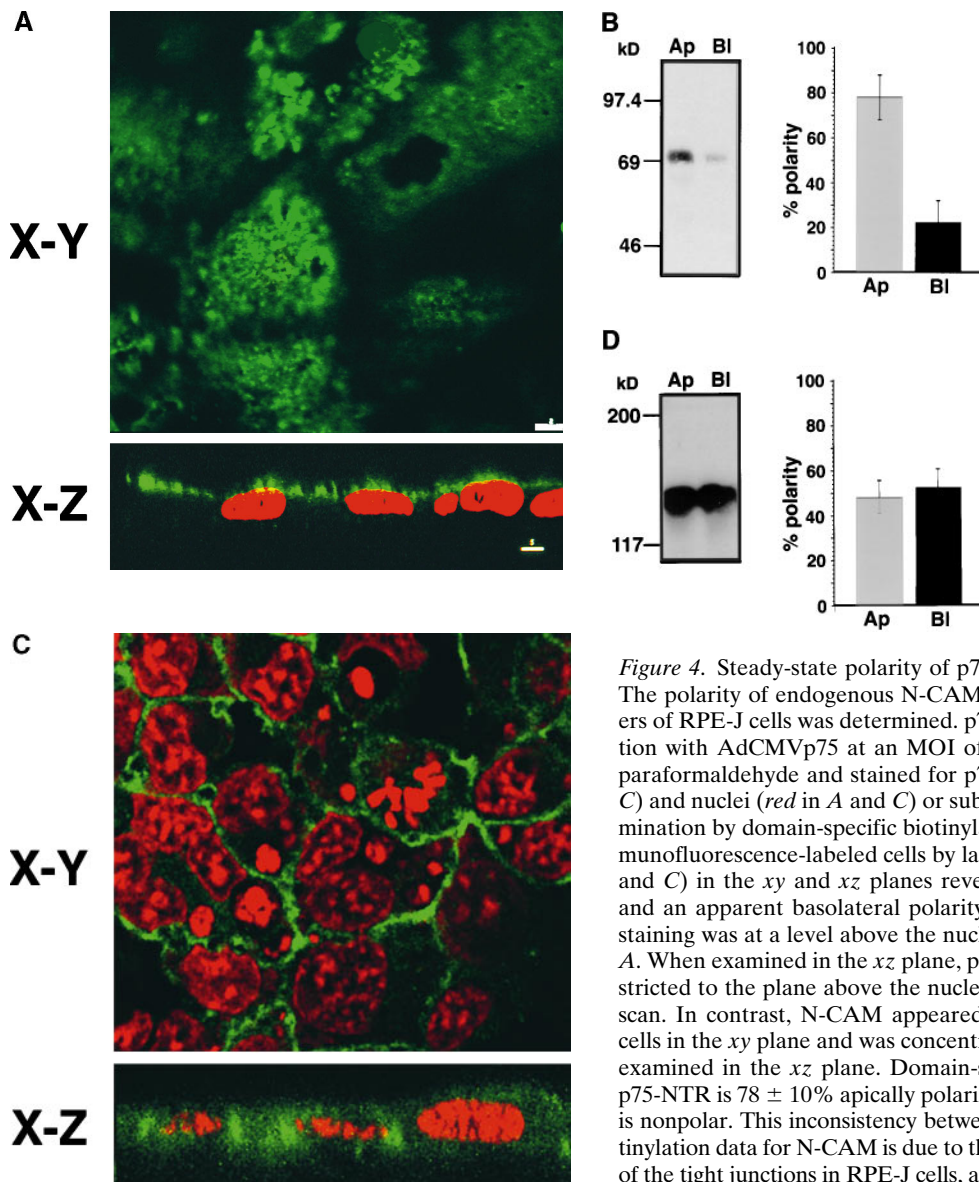| kD	Ap	Bl
200		
117		

C

X-Y

X-Z

Figure 4. Steady-state polarity of p75-NTR and N-CAM in RPE-J cells. The polarity of endogenous N-CAM or p75-NTR in confluent monolayers of RPE-J cells was determined. p75-NTR was introduced by transduction with AdCMVp75 at an MOI of 1–3. Cells were either fixed in 4% paraformaldehyde and stained for p75-NTR or N-CAM (*green* in *A* and *C*) and nuclei (*red* in *A* and *C*) or subjected to steady-state polarity determination by domain-specific biotinylation (*B* and *D*). Examination of immunofluorescence-labeled cells by laser scanning confocal microscopy (*A* and *C*) in the *xy* and *xz* planes revealed an apical polarity of p75-NTR and an apparent basolateral polarity of endogenous N-CAM. p75-NTR staining was at a level above the nuclei, as shown by the apical *xy* scan in *A*. When examined in the *xz* plane, p75-NTR staining was again found restricted to the plane above the nucleus as shown in the representative *xz* scan. In contrast, N-CAM appeared confined to the lateral surfaces of cells in the *xy* plane and was concentrated in the lateral membranes when examined in the *xz* plane. Domain-selective biotinylation confirms that p75-NTR is 78 ± 10% apically polarized (*B*), but it indicates that N-CAM is nonpolar. This inconsistency between the immunofluorescence and biotinylation data for N-CAM is due to the unusual medial–lateral localization of the tight junctions in RPE-J cells, as demonstrated in Fig. 3. Bars, 5 μm.

we have previously shown that, in RPE-J cells, influenza HA is delivered to the apical surface by an indirect pathway that involves the basolateral membrane, our results suggest that p75-NTR and influenza HA use different mechanisms for apical transport that can be discriminated by certain cells (e.g., RPE-J) but not by other epithelial cells (e.g., MDCK).

Surface Delivery of EMMPRIN and N-CAM in RPE-J Cells. We next determined the sites of initial surface delivery of endogenous EMMPRIN (Fig. 5, *D–F*) and N-CAM (Fig. 5, *G–I*). Newly synthesized EMMPRIN was detected at the cell surface as the mature 50–55-kD protein as early as ~1 h after synthesis, with a half-time of 90 min. A substantial amount of EMMPRIN never left the ER (Fig. 5 *D*, total). Most of the EMMPRIN that was transported to the plasma membrane was initially delivered to the basolateral surface (Fig. 5, *D–F*, surface panels). EMMPRIN continued to accumulate through the 4-h chase point, although the rate of accumulation slowed down between 2 and 4 h. N-CAM, in contrast, was targeted in near equal

amounts to both apical and basolateral surfaces as early as 30 min into the chase and remained nonpolar for the duration of each experiment (Fig. 5, *G–I*). Taken together with the experiments in Figs. 2 and 4, these results indicate that RPE-J cells resemble immature RPE in their sorting phenotype. The more apical localization of N-CAM in P0 RPE might be attributed to the apical position of the tight junction in this epithelium, combined with a 3:1 apical/basolateral surface area ratio.

Selective Suppression of Basolateral Signals by RPE

The asynchronous apical localization of N-CAM and EMMPRIN in maturing RPE in vivo and their differential targeting by cultured RPE-J monolayers suggests that RPE cells have the ability to selectively suppress decoding of basolateral signals. To investigate this hypothesis directly in vivo, truncated and chimeric N-CAMs were expressed in RPE by adenovirus-mediated gene transfer. Additional experiments demonstrated that EMMPRIN possesses a
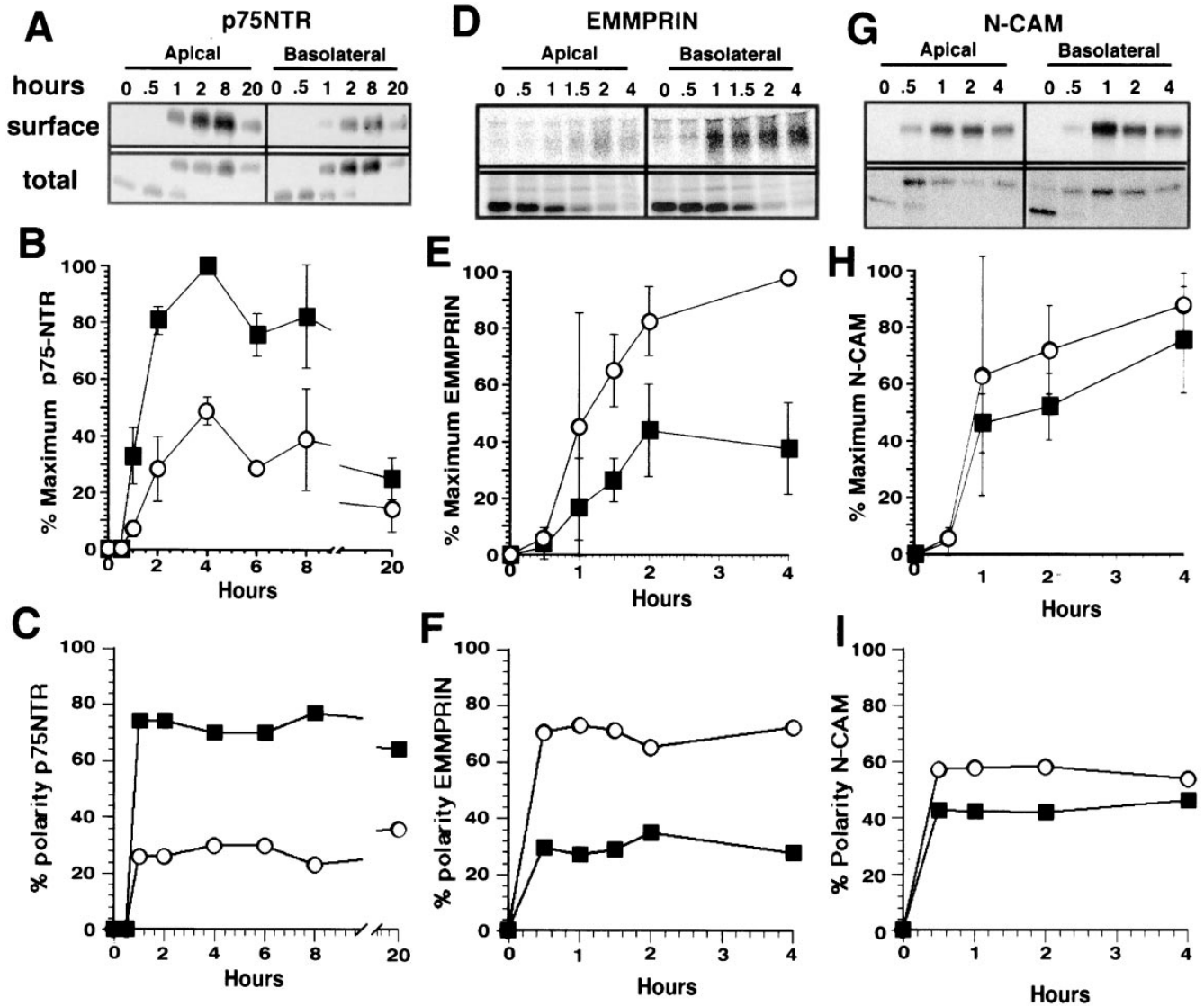
Figure 5. Targeting of p75-NTR, EMMPRIN, and N-CAM in RPE-J cells. The transport of endogenous EMMPRIN and N-CAM, or p75-NTR (expressed via transduction with AdCMVp75 at an MOI of 1–3) in confluent monolayers of RPE-J cells was determined. Targeting to the plasma membrane was determined by pulse chase analysis. The delivery of p75-NTR *(A–C)*, EMMPRIN *(D* and *E)*, and N-CAM *(G–I)* to the apical *(squares)* and basolateral *(circles)* surfaces of RPE-J cells was determined using pulse chase followed by domain-specific biotinylation. Samples were resolved by SDS-PAGE and fluorography *(A* and *G)* or phosphorimage analysis *(D)* and quantified using either densitometry *(B* and *H)* or phosphorimage analysis *(E)*. p75-NTR arrived at the cell surface between 1 and 2 h into the chase *(A–C)* at steady-state values *(C)*. EMMPRIN was first observed at the cell surface at 30 min *(E)* in very small amounts, becoming reliably detectable by 60–90 min. A basolateral distribution of EMMPRIN was immediately obtained upon arrival at the cell surface, indicating direct basolateral targeting. N-CAM was first detected 30 min into the chase *(H)*, and consistent with its measured steady-state polarity, it was not delivered with a clear preference to either surface *(H* and *I)*. Values in *B*, *E*, and *H* are mean ± SD from three separate experiments. The large error bars at early time points in *E* and *H* are due to low levels of detectable protein. Polarity values in *C*, *F*, and *I* are derived from the means shown in *B*, *E*, and *H*. In no experiment did the delivery of EMMPRIN to the apical surface exceed the delivery to the basolateral surface at early time points.

basolateral signal that is recognized by MDCK cells and RPE-J cells but appears to be ignored by adult rat RPE.

The N-CAM Basolateral Targeting Signal Is Not Recognized by RPE-J Cells or RPE In Vivo. N-CAM contains a dominant basolateral sorting signal in its cytoplasmic domain (Le Gall et al., 1997). When fused to the COOH-terminal end of truncated p75-NTR lacking the cytoplasmic domain, this 40–amino acid signal overcomes apical infor-

mation in the ectodomain of p75-NTR and reverses its polarity from apical to basolateral in MDCK cells (Le Gall et al., 1997). Since N-CAM was nonpolar in RPE-J cells and apical in RPE cells in vivo, we examined the localization of a truncated form of N-CAM (N-CAM749t), which lacks the basolateral targeting signal, as well as a chimera of p75-NTR transmembrane and ectodomains with the N-CAM basolateral sorting signal (p75 + Bl). An adenovirus vec-
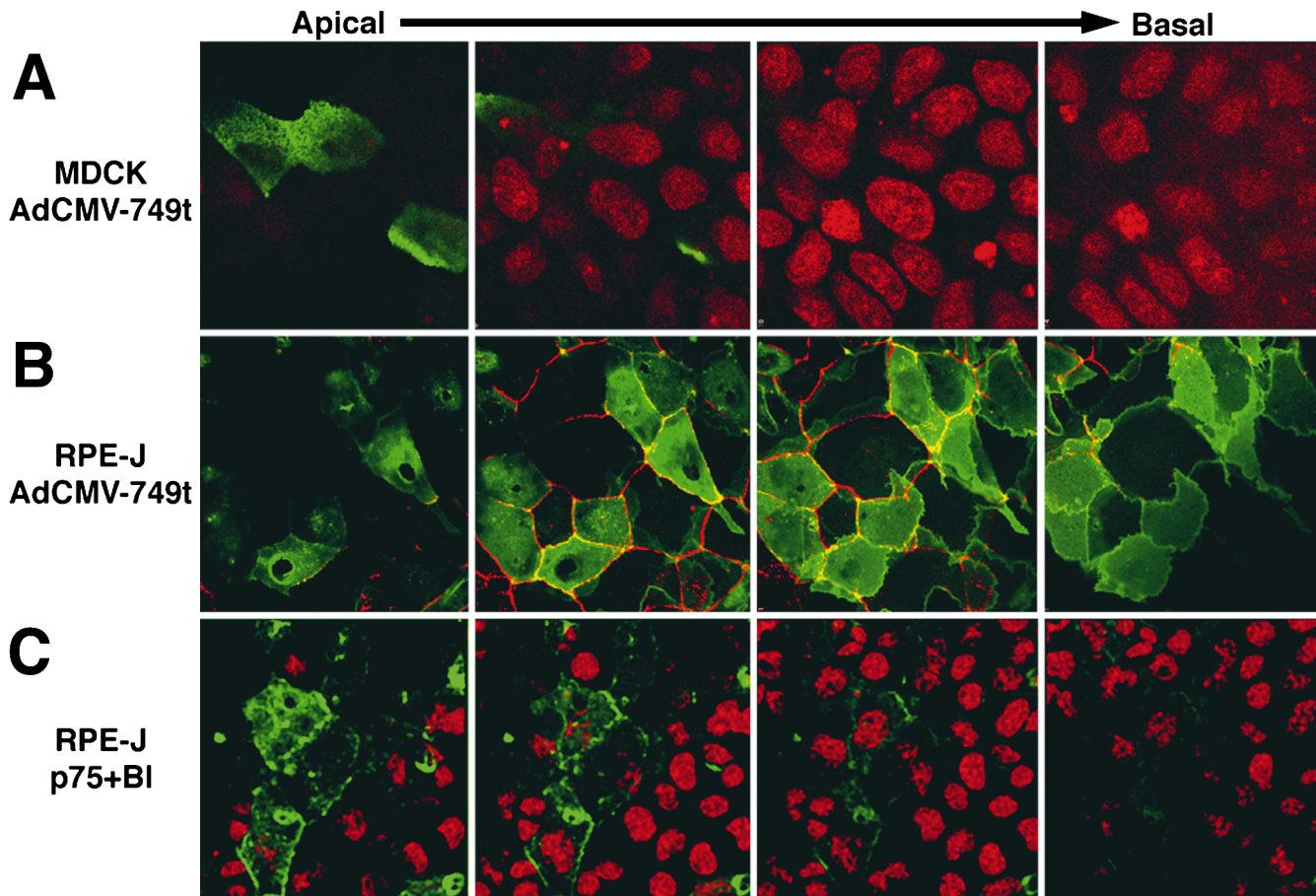
Figure 6. RPE-J cells do not recognize a sorting signal in N-CAM: confocal microscopy. MDCK (*A*) and RPE-J (*B* and *C*) cells were transduced with AdCMV-749t (*A* and *B*), a replication-defective adenovirus vector driving expression of N-CAM749t under control of a CMV promoter, or stably transfected (*C*) with p75-NTR fused to the N-CAM basolateral sorting signal (p75 + Bl). Cells were fixed and then stained for N-CAM with monoclonal antibody 5e (*green*). Nuclei in *A* and *C* were stained with propidium iodide (*red*). RPE-J cells transduced with AdCMV-749t (*B*) were stained with ZO-1 (*red*) rather than propidium iodide to facilitate localization of the tight junctions. The polarity of N-CAM749t was determined from serial optical sections using confocal microscopy. Cells were sectioned in the *xy* plane from the apical to basal surfaces in 0.3-μm increments. The planes are shown at a 1.2-μm interval. As predicted from previously published work, N-CAM749t is apically polarized in MDCK cells. Interestingly, N-CAM749t, like wild-type N-CAM (see Fig. 4), is nonpolar in RPE-J cells as judged by its distribution above, within, and below planes containing ZO-1 staining. In RPE-J cells expressing p75 + Bl, the predominant staining was in apical sections, further confirming that RPE-J cells do not recognize the basolateral sorting signal in N-CAM. Data in *C* are representative of that obtained from two independent clones.

tor (AdCMV-749t) was produced to express N-CAM749t, and p75 + Bl in the plasmid pCB7 was stably transfected into RPE-J cells.

As predicted by transfection experiments, N-CAM749t exhibited an apical steady-state polarity in MDCK cells transduced with AdCMV-749t when examined by either confocal microscopy (Fig. 6 *A*) or domain-selective biotinylation (data not shown). However, when expressed in RPE-J cells, N-CAM749t displayed a clearly nonpolar distribution as determined by confocal microscopy (Fig. 6 *B*). This was further confirmed by domain-selective biotinylation (Fig. 7 *B*). We next examined two clones of RPE-J cells stably transfected with p75 + Bl. Confocal microscopy indicated an apical localization (Fig. 6 *C*), which was further confirmed by domain-selective biotinylation (Fig. 7 *A*). Thus, RPE-J cells read neither the N-CAM basolateral signal nor apical information present in the ectodomain of N-CAM.

One possible explanation of these data is that RPE interprets N-CAM's basolateral targeting signal as an apical targeting signal. To test this hypothesis, we transduced N-CAM749t into RPE by injection of AdCMV-749t into the subretinal space of adult and newborn (P0) rat eyes. Inspection of neural retina–free cryosections (Fig. 8) at either P2 or 5 d after injection in the adult eye demonstrated an apical localization of N-CAM749t, identical to that of full-length endogenous N-CAM (compare Fig. 8 with Fig. 2, *H* and *L*). These experiments demonstrate that RPE cells in vivo cannot recognize the basolateral sorting signal of N-CAM.

EMMPRIN Contains a Basolateral Sorting Signal. Previous studies have established the basolateral distribution of EMMPRIN in a multitude of extraocular epithelia; however, no information is available on which domain of this type I protein contains basolateral information. To determine the domain localization of EMMPRIN's basolateral
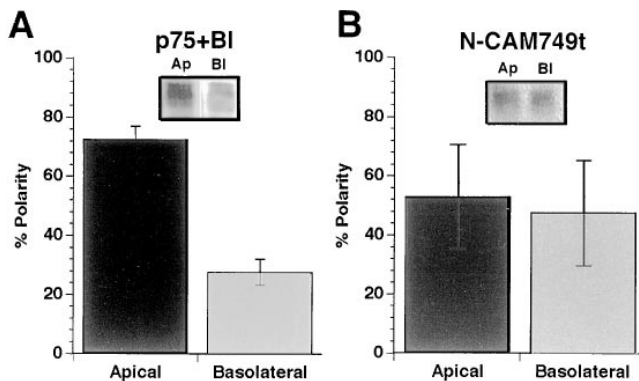
Figure 7. RPE-J cells do not recognize a sorting signal in N-CAM: domain-selective biotinylation. RPE-J cells transfected with p75+Bl or transduced with AdCMV-749t were subjected to domain-selective biotinylation to confirm the steady-state polarity data obtained from confocal microscopy. As predicted, p75+Bl (*A*) was 74 ± 4% apically polarized, similar to the 78% apical polarity obtained for wild-type p75-NTR (see Fig. 6). Like endogenous full-length N-CAM, N-CAM749t was not polarized by RPE-J cells, confirming the data obtained by confocal microscopy, and implying that the polarity of N-CAM in RPE-J cells is not dependent upon sorting in the TGN.
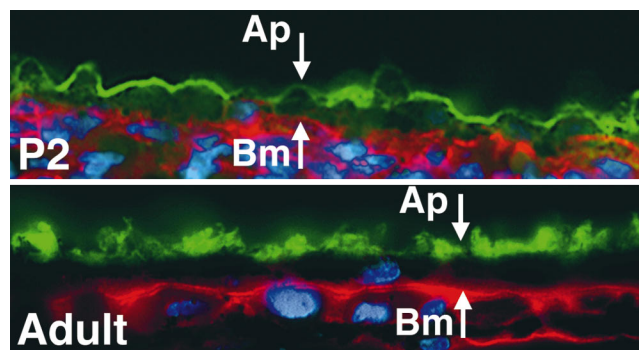

Figure 8. Steady-state polarity of N-CAM749t in RPE in situ. P0 or adult rats were injected subretinally with AdCMV-749t as described in Materials and Methods. At P2 or 5 d after injection for adults, animals were killed, and their eyes were processed for immunofluorescence microscopy. Cryosections were stained with monoclonal antibody 5e against chicken N-CAM (*green*), a polyclonal antibody against laminin (*red*), and DAPI (nuclei in *blue*). The clear separation of the N-CAM from laminin staining in both P2 and adult eyes indicates that the N-CAM basolateral targeting signal does not contribute to the apical polarity of N-CAM in RPE cells in situ.

signal, we established MDCK cell lines stably expressing EMMPRIN, a cytoplasmic truncation mutant lacking all but the two juxtamembrane amino acids (EMMPRIN-244t), and a secreted form lacking both cytoplasmic and transmembrane domains (EMMPRIN-203t). Domain-specific biotinylation confirmed that transfected EMMPRIN was predominantly basolateral at steady state, ranging from 82–94% in the three clones examined (Fig. 9 *A*). In contrast, EMMPRIN-244t was not polarized in three independent MDCK clones, as determined by both confocal microscopy and domain-selective biotinylation (Fig. 9 *B*), indicating that the cytoplasmic tail contains a basolateral signal.

To determine the site of initial surface delivery of EMMPRIN in MDCK cells, we used a pulse-chase protocol combined with immune and streptavidin precipitation (Fig. 10). Newly synthesized EMMPRIN was detected at the cell surface as a mature 50–55-kD protein as early as ~1 h after synthesis, with a half-time of 90 min. EMMPRIN continued to accumulate through the 4-h chase point, although the rate of accumulation slowed down between 2 and 4 h. Two clones of MDCK cells expressing EMMPRIN-203t released pulse-labeled protein preferentially (60–70%) into the apical medium, starting 60 min into the chase, consistent with the presence of a weak apical signal. Taken together, these data are consistent with the presence of a dominant basolateral sorting signal in EMMPRIN's cytoplasmic domain.

Discussion

For functional reasons not yet fully understood, the mature RPE must place on its apical surface certain proteins that are cognate basolateral markers in other epithelia. A combination of in vivo and in vitro studies reported in this paper provides novel information on the mechanisms in-

volved in this process. The first group of experiments studied the effect of the establishment of mature RPE–neural retina contacts in the developing postnatal rat retina on the polarized distribution of two basolateral markers and one apical marker (as defined by their behavior in general epithelia). The primary observation was that whereas the RPE kept the well-characterized apical marker p75-NTR on the apical surface at all times after birth, it handled the two "basolateral" markers differently. While the maturing RPE localized N-CAM-140 continually on the apical surface, exactly as p75-NTR, overriding a dominant basolateral signal previously defined in MDCK cells (Le Gall et al., 1997), it shifted EMMPRIN progressively from a basolateral to an apical distribution during the first 10 d of postnatal development. The sorting of p75-NTR and EMMPRIN to opposite domains of the plasma membrane, a phenotype similar to that of MDCK cells, was reproduced by the RPE cell line RPE-J (see below). Since independent morphological studies showed that the basolateral surface of RPE cells constitutes 27% of the total plasma membrane at P2, an important corollary of these experiments is that low-fidelity basolateral sorting by immature RPE is sufficient to concentrate EMMPRIN severalfold at the basolateral membrane. A low-fidelity basolateral sorting of EMMPRIN was indeed observed in the RPE-J cell line (Fig. 4, *D–F*). A second major corollary of this group of in vivo experiments is that RPE cells can discriminate between the basolateral signals of N-CAM-140 and EMMPRIN, suggesting that any intersection of these molecules in the basolateral pathway must take place after sorting has occurred.

One important question raised by these initial studies was whether the apical localization of cognate basolateral markers in RPE depends on active recognition of sorting signals in the transported protein or is a passive process that does not require sorting signals. Subsequent experiments were designed to attempt to answer this question.
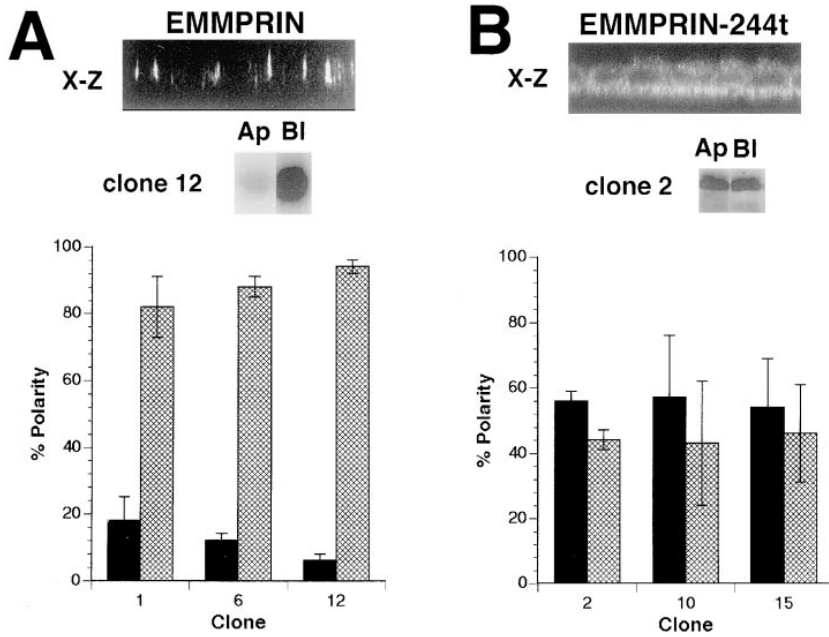
A EMMPRIN

X-Z

B EMMPRIN-244t

X-Z

Figure 9. The cytosolic domain of EMMPRIN contains basolateral sorting information. MDCK cells were stably transfected with either pBk-EMMPRIN (*A*) or pBk-EMMPRIN-244t (*B*). Clones were isolated, and the polarity of EMMPRIN or EMMPRIN-244t was determined by either confocal microscopy or domain-selective biotinylation. The confocal micrographs in *A* and *B* are representative vertical scans in the *xz* planes of the clone indicated in the accompanying streptavidin blot. Graphs indicate data from three separate clones where data are mean $\pm$ SD, $n > 3$. EMMPRIN was basolaterally polarized while EMMPRIN-244t was distinctly nonpolar in all clones examined.

RPE Cells Do Not Recognize Basolateral Signals in N-CAM or EMMPRIN

We considered two possible scenarios that would explain our findings. In the first scenario, the RPE cannot recognize basolateral information in N-CAM or EMMPRIN, except for a brief period after birth for the latter. In the second scenario, the RPE interprets the basolateral signals of both proteins as apical signals, and therefore, the apical localization of the proteins depends on the presence of these signals. Several pieces of evidence support the first scenario.

(a) Morphometric Analysis of Adult RPE Demonstrated an Apical/Basolateral Surface Ratio of ~3:1. This ratio (73% apical, Table I; Fig. 3) is identical to the apical polarity of

EMMPRIN in adult RPE (74% or ~3:1 apical), as quantified in eyecups by a modified biotin assay (Marmorstein et al., 1996), indicating that the concentration of EMMPRIN is uniform throughout the entire plasma membrane. This experiment suggests that no active concentrative process is required to generate an apical distribution of this protein.

(b) Although the Apical Surface of RPE Expands Considerably between P2 and Adulthood, the Basolateral Membrane Expands Proportionally, Resulting in a Constant ~3:1 Apical/Basolateral Ratio. This result excludes the possibility that the apical polarization of EMMPRIN is merely the consequence of the expansion of the apical surface relative to the basolateral surface. Taken together with other data, it suggests that an active basolateral sorting mechanism is
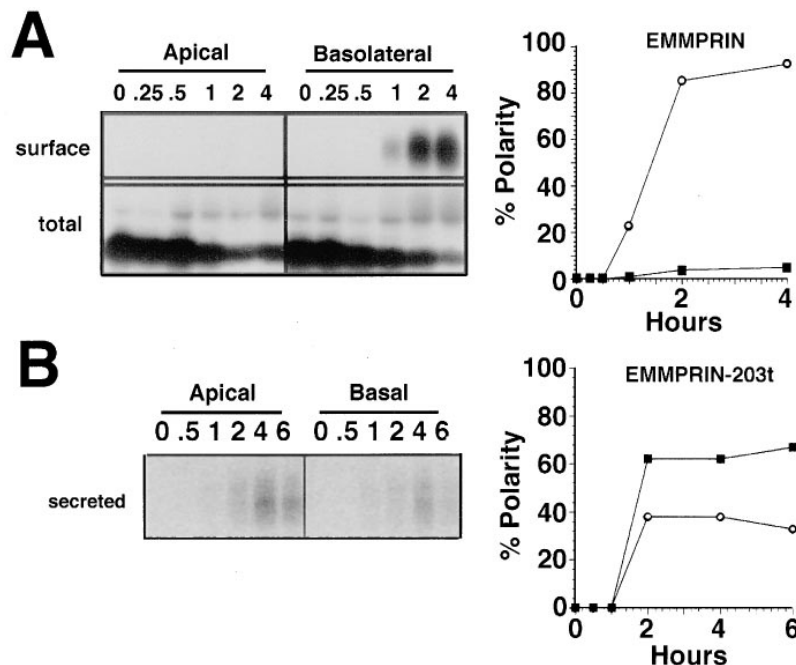

Figure 10. Post-Golgi delivery of EMMPRIN and EMMPRIN-203t. The delivery of EMMPRIN to the surface of confluent MDCK monolayers grown on Transwell filters was determined by pulse chase followed by domain-specific biotinylation. Biotinylated cells were lysed, and EMMPRIN was immunoprecipitated. The immunoprecipitates were eluted from protein A–Sepharose, and 10% of the sample was retained for totals (*A*). Surface EMMPRIN was obtained from the remaining 90% of the sample by precipitation with streptavidin Sepharose. EMMPRIN arrived at the basolateral surface of stably transfected MDCK cells between 1 and 2 h into the chase with a half-time of surface delivery of ~90 min. The steady-state values were obtained immediately upon arrival at the cell surface for MDCK cells. The appearance of EMMPRIN in the media of MDCK cells transfected with EMMPRIN-203t (*B*) was slower than for the wild-type EMMPRIN appearing at steady-state levels predominantly in the apical media 2 h into the chase.

required to sort the protein basolaterally at P0 and that mature RPE cells suppress EMMPRIN's basolateral signal. In addition, this result is consistent with a passive mechanism mediating the apical localization of N-CAM at birth and in adult RPE.

(c) RPE-J Cells Recognize Basolateral Information in EMMPRIN but Not in N-CAM-140. We have previously shown that the RPE-J cell line preserves important characteristics of native RPE, such as the ability to sort influenza HA via a transcytotic pathway (Bonilha et al., 1997) and the phagocytic mechanism for rod outer segments (Finnemann et al., 1997*b*). Protein targeting experiments in this report showed that RPE-J cells sort EMMPRIN intracellularly into a basolateral pathway, albeit less accurately than MDCK cells. On the other hand, RPE-J cells failed to sort N-CAM intracellularly and delivered this protein in equal amounts to both surfaces during biogenesis. Since morphometric analysis demonstrated a 1:1 apical/basolateral surface area ratio, the nonpolar delivery of N-CAM explains its nonpolar distribution regarding the plane of the tight junction, measured by a steady-state biotin polarity assay. These experiments demonstrated that the sorting phenotype of RPE-J cells is similar to that of immature RPE cells, from which they were originally immortalized by transfection of SV-40 T antigen (Nabi et al., 1993).

(d) N-CAM's Basolateral Signal Is Not Interpreted as an Apical Localization Signal in Adult RPE. To test the hypothesis that basolateral signals might be interpreted as apical targeting signals by RPE, we constructed a replication-defective adenovirus expressing a mutant N-CAM devoid of its basolateral sorting signal (N-CAM749t) and introduced it into RPE by subretinal injection. N-CAM749t was expressed apically in both P2 and adult RPE, indicating that the cognate basolateral signal was not required for apical targeting in vivo. Furthermore, N-CAM749t, like endogenous N-CAM, was nonpolar in RPE-J cells, indicating that these cells did not recognize any recessive apical signal in this protein. Finally, the basolateral sorting signal in N-CAM failed, when fused to truncated p75-NTR, to redirect the protein to the basolateral surface of transfected RPE-J cells. Taken together, these data strongly imply that RPE cells neither interpret N-CAM's basolateral signal as an apical targeting signal nor recognize any other putative apical targeting signals in this molecule.

The experiments discussed above strongly suggest that adult RPE cells do not use any sorting information in N-CAM to localize it to the apical surface. A similar "passive" localization mechanism is likely to be responsible for the apical localization of EMMPRIN in adult RPE; however, additional experiments are still required to demonstrate this point. It is unclear at the moment whether the inability of adult RPE to recognize basolateral signals is caused by tissue-specific downregulation of critical components of the basolateral targeting machinery (e.g., a specific adaptor complex that promotes the assembly of basolateral vesicles from the TGN), by inactivation of the basolateral sorting signal (e.g., by phosphorylation), or by other mechanisms. Since cognate apical sorting signals in N-CAM and EMMPRIN are not recognized by RPE (see next section for discussion of this point), our data support a model in which the apical polarity of these proteins does not result from selective, signal-mediated incorporation into either apical or basolateral post-Golgi transport vesicles. Of course, our results do not discard the possibility that the apical localization of these proteins may be enhanced by stabilization through binding to components of the IPM or of the neural retina.

Selective Decoding of Apical Sorting Signals by RPE

The data presented in this report also exclude the possibility that RPE may recognize strong apical sorting signals in either N-CAM or EMMPRIN. Of the apical targeting signals described to date, only *N*-glycans (Scheiffele et al., 1995) are present in these two proteins. Recent results from our laboratory indicate that *N*-glycans in N-CAM are not effective apical sorting signals in MDCK cells (Yeaman et al., 1997). Finally, mutant forms of N-CAM and EMMPRIN devoid of their basolateral signals are poorly targeted in RPE-J and/or MDCK cells (Figs. 4–10).

On the other hand, RPE cells recognize apical sorting information in p75-NTR, as indicted by the accurate apical targeting of this molecule after adenovirus-mediated transduction into RPE-J cells (Fig. 8). This is in spite of an apical/basolateral surface area ratio of 1:1 in these cells (Fig. 3 and Table I). The rapid intracellular sorting and vectorial apical delivery of p75-NTR in RPE-J cells contrasts with the slow transcytotic pathway followed by influenza HA (Bonilha et al., 1997). Clearly, influenza HA and p75-NTR use different targeting mechanisms to reach the apical surface of RPE-J cells. However, in MDCK cells both proteins are targeted vectorially to the apical surface with identical fast kinetics (Rodriguez-Boulan and Nelson, 1989; Yeaman et al., 1997). An important conclusion of these experiments in RPE-J cells is that, by demonstrating a dissociation of the apical delivery routes of two cognate apical markers, they uncover two distinct apical targeting systems that cannot be discerned in MDCK cells. Additional data from the literature support the idea that these two proteins are sorted apically by different mechanisms. Apical targeting of influenza HA appears to require the interaction of specific sequences in the transmembrane domain (Scheiffele et al., 1997) with detergent insoluble lipid "rafts" in the Golgi apparatus (Yoshimori et al., 1996; Simons and Ikonen, 1997). On the other hand, p75-NTR does not become detergent insoluble at any point during its biogenesis (Le Bivic, A., personal communication), and the apical signal of p75-NTR is located in its *O*-glycosylated stem, a structure not present in HA (Yeaman et al., 1997). The experiments reported here suggest that RPE-J cells may recognize the *O*-glycosylated stem of p75-NTR, but not the transmembrane domain of HA as a signal for incorporation into TGN transport vesicles destined for fusion with the apical membrane.

Towards Understanding the Flexible Epithelial Phenotype: Gene Transfer Studies in Native Epithelia

Several reports from various laboratories have highlighted the remarkable ability of different epithelial cell types to customize the distribution of their apical and basolateral plasma membrane proteins to their own specific needs (for reviews see Rodriguez-Boulan and Powell, 1992; Keller and Simons 1997). Typically, different epithelial cells may localize a given protein to different surfaces, thus blurring

the definition of a protein as apical or basolateral. This has been shown for Na,K-ATPase (Gundersen et al., 1991), N-CAM (Gundersen et al., 1993), EMMPRIN/RET-PE2 (Marmorstein et al., 1996; Finnemann et al., 1997), LDL receptor (Pathak et al., 1990), GPI-proteins (Zurzolo et al., 1993), the anion transporter (van Adelsberg, 1994), and some proteins carrying basolateral tyrosine-motifs (Courtois-Coutry et al., 1997). A variation of the "flexible phenotype" theme is to target a given protein (usually an apical marker) to its final site of residence using two alternative routes, either direct transport from the TGN or an indirect transcytotic pathway. This has been shown for DPPase IV in various epithelial cell lines and hepatocytes (Bartles et al., 1987; Casanova et al., 1991; Zurzolo et al., 1992) and for HA in MDCK vs. RPE (Bonilha et al., 1997). The mechanisms responsible for this "flexibility" or "plasticity" of the epithelial phenotype are largely unidentified. Al-Awqati and coworkers have recently postulated an important role for an extracellular matrix protein, named Hensin, in the regulation of the polarized distribution of the anion transporter in kidney-collecting duct cells (van Adelsberg et al., 1994; Takito et al., 1996), but the exact mechanism involved in the polarity reversal remains unknown.

Even when sorting signals have been identified that guide proteins to apical and basolateral locations, practically all of these signals have been defined in MDCK cells. Since the final localization of a protein depends on how its specific complement of apical and basolateral signals is hierarchically recognized by the sorting mechanisms in the host cell, much work is still needed to determine how individual epithelial cell types (particularly native epithelia) define their characteristic sorting phenotypes. This is a necessary first step in the attempt to identify the molecular bases of the phenotypic variation between different epithelia.

The experiments in this report constitute the first systematic approach to use gene transfer protocols in vivo to study the sorting phenotype of a native mammalian epithelium. They focus on the RPE, a remarkable epithelium that differs from most simple epithelia in that its apical surface is not free but performs important interactive functions with a second cell type, the retinal photoreceptors. The data precisely define developmental stage-specific differences and similarities in the ability to recognize basolateral and apical signals between RPE and the prototype MDCK cell line. These experiments open the way towards the identification of molecules involved in cell type specific variation in polarized sorting processes. Current work in our laboratory aims to identify specific components of the basolateral sorting machinery that may be absent or altered in RPE cells.

References

Bartles, J.R., L.T. Braiterman, and A.L. Hubbard. 1985*a*. Biochemical characterization of domain-specific glycoproteins of the rat hepatocyte plasma membrane. *J. Biol. Chem.* 260:12792–12802.

Bartles, J.R., T. Braiterman, and A.L. Hubbard. 1985*b*. Endogenous and exogenous domain markers of the rat hepatocyte plasma membrane. *J. Cell Biol.* 100:1126–1138.

Bartles, J.R., H.M. Feracci, B. Stieger, and A.L. Hubbard. 1987. Biogenesis of the rat hepatocyte plasma membrane in vivo: comparison of the pathways taken by apical and basolateral proteins using subcellular fractionation. *J. Cell Biol.* 105:1241–1251.

Biswas, C., Y. Zhang, R. De Castro, H. Guo, T. Nakamura, H. Kataoka, and K. Nabeshima. 1995. The human tumor cell-derived collagenase stimulatory factor (renamed EMMPRIN) is a member of the immunoglobulin superfamily. *Cancer Res.* 55:434–439.

Bok, D. 1982. Autoradiographic studies on the polarity of plasma membrane receptors in RPE cells. *In* Structure of the Eye. J. Hollyfield, editor. Elsevier North Holland, New York. 247–256.

Bonilha, V.L., A.D. Marmorstein, L. Cohen-Gould, and E. Rodriguez-Boulan. 1997. Apical sorting of hemagglutinin by transcytosis in retinal pigment epithelium. *J. Cell Sci.* 110:1717–1727.

Braekevelt, C.R., and M.J. Hollenberg. 1970. Development of the retinal pigment epithelium, choriocapillaris, and Bruch's membrane in the albino rat. *Exp. Eye Res.* 9:124–131.

Butor, C., and J. Davoust. 1992. Apical to basolateral surface area ratio and polarity of MDCK cells grown on different supports. *Exp. Cell Res.* 203:115–127.

Casanova, J.E., Y. Mishumi, Y. Ikehara, A.L. Hubbard, and K.E. Mostov. 1991. Direct apical sorting of rat liver dipeptidylpeptidase IV expressed in Madin-Darby kidney cells. *J. Biol. Chem.* 266:24428–24432.

Courtois-Coutry, N., D. Roush, V. Rajendran, J.B. McCarthy, J. Geibel, M. Kashgarian, and M.J. Caplan. 1997. A tyrosine-based signal targets H/K-ATPase to a regulated compartment and is required for the cessation of gastric acid secretion. *Cell.* 90:501–510.

Dowling, J.E., and I.R. Gibbons. 1962. The fine structure of the pigment epithelium in the albino rat. *J. Cell Biol.* 14:459–474.

Finnemann, S.C., A.D. Marmorstein, J.M. Neill, and E. Rodriguez-Boulan. 1997*a*. Identification of the retinal pigment epithelium protein RET-PE2 as CE-9/OX-47, a member of the immunoglobulin superfamily. *Invest. Ophthalmol. Vis. Sci.* 38:2366–2374.

Finnemann, S.C., V.L. Bonilha, A.D. Marmorstein, and E. Rodriguez-Boulan. 1997*b*. Phagocytosis of rod outer segments by retinal pigment epithelial cells requires αvβ5 integrin for binding but not internalization. *Proc. Natl. Acad. Sci. USA.* 94:12932–12937.

Gallemore, R.P., B.A. Hughs, and S.S. Miller. 1997. Retinal pigment epithelial transport mechanisms and their contributions to the electroretinogram. *Prog. Retinal Eye Res.* 16:509–566.

Graham, F., and A. Van der Eb. 1973. A new technique for the assay of infectivity of human adenovirus 5 DNA. *Virology.* 52:456–467.

Gundersen, D., J. Orlowski, and E. Rodriguez-Boulan. 1991. Apical polarity of Na,K-ATPase in retinal pigment epithelium is linked to a reversal of the ankyrin-fodrin submembrane cytoskeleton. *J. Cell Biol.* 112:863–872.

Gundersen, D., S.K. Powell, and E. Rodriguez-Boulan. 1993. Apical polarization of N-CAM in retinal pigment epithelium is dependent on contact with the neural retina. *J. Cell Biol.* 121:335–343.

Guo, H., S. Zucker, M.K. Gordon, B.P. Toole, and C. Biswas. 1997. Stimulation of matrix metalloproteinase production by recombinant extracellular matrix metalloproteinase inducer from transfected chinese hamster ovary cells. *J. Biol. Chem.* 272:24–27.

Hanzel, D., I.R. Nabi, C. Zurzolo, S.K. Powell, and E. Rodriguez-Boulan. 1991. New techniques lead to advances in epithelial cell polarity. *Semin. Cell Biol.* 2:341–353.

Johnson, L.V., G.S. Hageman, and J.C. Blanks. 1986. Interphotoreceptor matrix domains ensheathe vertebrate cone photoreceptor cells. *Invest. Ophthalmol. Vis. Sci.* 27:129–135.

Keller, P., and K. Simons. 1997. Post-Golgi biosynthetic trafficking. *J. Cell Sci.* 110:3001–3009.

Laemmli, U.K. 1970. Cleavage of structural proteins during the assembly of the head of bacteriophage T4. *Nature.* 227:680–685.

Landers, R.A., A. Tarawa, H.H. Verner, and J.G. Hollyfield. 1991. Proteoglycans in the mouse interphotoreceptor matrix. IV. Retinal synthesis of chondroitin sulfate proteoglycan. *Exp. Eye Res.* 52:65–74.

Le Bivic, A., Y. Sambuy, A. Patzak, N. Patil, M. Chao, and E. Rodriguez-Boulan. 1991. An internal deletion in the cytoplasmic tail reverses the apical localization of human NGF receptor in transfected MDCK cells. *J. Cell Biol.* 115:607–618.

Le Gall, A.H., S.K. Powell, C.A. Yeaman, and E. Rodriguez-Boulan. 1997. The neural cell adhesion molecule expresses a tyrosine independent basolateral

sorting signal. *J. Biol. Chem.* 272:4559–4567.

Marmorstein, A.D., V.L. Bonilha, S. Chiflet, J.M. Neill, and E. Rodriguez-Boulan. 1996. The polarity of the plasma membrane protein RET-PE2 in the retinal pigment epithelium is developmentally regulated. *J. Cell Sci.* 109:3025–3034.

Marmorstein, A.D., C. Zurzolo, A. Le Bivic, and E. Rodriguez-Boulan. 1998. Cell surface biotinylation techniques and determination of protein polarity. *In* Cell Biology: A Laboratory Handbook. Vol. 4. J.E. Celis, editor. Academic Press, New York. 341–350.

Miller, S.S., and R. Steinberg. 1977. Passive ionic properties of frog retinal pigment epithelium. *J. Membr. Biol.* 36:337–372.

Monlauzeur, L., A. Rajasekaran, M. Chao, E. Rodriguez-Boulan, and A. Le Bivic. 1995. A cytoplasmic tyrosine is essential for the basolateral localization of mutants of the human nerve growth factor receptor in Madin-Darby canine kidney cells. *J. Biol. Chem.* 270:12219–12225.

Nabi, I.R., A.P. Mathews, L. Cohen-Gould, D. Gundersen, and E. Rodriguez-Boulan. 1993. Immortalization of polarized rat retinal pigment epithelium. *J. Cell Sci.* 104:37–49.

Okami, T., A. Yamamoto, K. Omori, T. Takada, M. Uyama, and Y. Tashiro. 1990. Immunocytochemical localization of Na,K-ATPase in rat retinal pigment epithelial cells. *J. Histochem. Cytochem.* 38:1267–1275.

Olney, J.W. 1968. An electron microscopic study of synapse formation, receptor outer segment development, and other aspects of developing mouse retina. *Invest. Ophthalmol.* 7:250–268.

Padgett, L.C., G. Lui, Z. Werb, and M.M. LaVail. 1997. Matrix metalloproteinase-2 and tissue inhibitor of metalloproteinase-1 in the retinal pigment epithelium and interphotoreceptor matrix: vectorial secretion and regulation. *Exp. Eye Res.* 64:927–938.

Pathak, R.K., M. Yokode, R.E. Hammer, S.L. Hofmann, M.S. Brown, J.L. Goldstein, and R.G.W. Anderson. 1990. Tissue-specific sorting of the human LDL receptor in polarized epithelia of transgenic mice. *J. Cell Biol.* 111:347–359.

Plantner, J.J., A. Smine, and T.A. Quinn. 1998. Matrix metalloproteinases and metalloproteinase inhibitors in human interphotoreceptor matrix and vitreous. *Curr. Eye Res.* 17:132–140.

Powell, S.K., B.A. Cunningham, G.M. Edelman, and E. Rodriguez-Boulan. 1991. Targeting of transmembrane and GPI-anchored forms of N-Cam to opposite domains of a polarized epithelial cell. *Nature.* 353:76–77.

Ratto, G., D. Robinson, B. Yan, and P. McNaughton. 1991. Development of the light response in neonatal mammalian rods. *Nature.* 351:654–657.

Rizzolo, L.J. 1990. The distribution of Na+, K+-ATPase in the retinal pigmented epithelium from chicken embryo is polarized in vivo but not in primary cell culture. *Exp. Eye Res.* 51:435–446.

Rizzolo, L.J. 1997. Polarity and the development of the outer blood-retinal barrier. *Histol. Histopath.* 12:1057–1067.

Rizzolo, L.J., and M. Heiges. 1991. The polarity of the retinal pigment epithelium is developmentally regulated. *Exp. Eye Res.* 53:549–553.

Rizzolo, L.J., and S. Zhou. 1995. The distribution of Na, K-ATPase and 5A11 antigen in apical microvilli of the retinal pigment epithelium is unrelated to α-spectrin. *J. Cell Sci.* 108:3623–3633.

Rizzolo, L.J., S. Zhou, and Z.Q. Li. 1994. The neural retina maintains integrins in the apical membrane of RPE early in development. *Invest. Opthalmol.*

Vis. Sci. 35:2567–2576.

Rodriguez-Boulan, E., and W.J. Nelson. 1989. Morphogenesis of the polarized epithelial cell phenotype. *Science.* 245:718–725.

Rodriguez-Boulan, E., and S.K. Powell. 1992. Polarity of epithelial and neuronal cells. *Annu. Rev. Cell Biol.* 8:395–427.

Scheiffele, P., J. Peranen, and K. Simons. 1995. N-glycans as apical sorting signals in epithelial cells. *Nature.* 378:96–98.

Scheiffele, P., M.G. Roth, and K. Simons. 1997. Interaction of influenza virus hemagglutinin with sphingolipid-cholesterol membrane rafts via its transmembrane domain. *EMBO (Eur. Mol. Biol. Organ.) J.* 16:5501–5508.

Simons, K., and E. Ikonen. 1997. Functional rafts in cell membranes. *Nature.* 387:569–572.

Spector, D.L., R.D. Goldman, and L.A. Leinwand. 1997. Cells: A Laboratory Manual. Vol. 2. Cold Spring Harbor Laboratory Press, Cold Spring Harbor, NY. 90.1–90.28.

Sullivan, D.M., D.C. Chung, E. Anglade, R.B. Nussenblatt, and K.C. Csaky. 1996. Adenovirus mediated gene transfer of ornithine aminotransferase in cultured human RPE. *Invest. Ophthalmol. Vis. Sci.* 37:768–774.

Takito, J., C. Hikita, and Q. Al-Aqwati. 1996. Hensin, a new collecting duct protein involved in the in vitro plasticity of intercalated cell polarity. *J. Clin. Invest.* 98:2324–2331.

Tawara, A., H.H. Verner, and J.G. Hollyfield. 1989. Proteoglycans in the mouse interphotoreceptor matrix. II. Origin and development of proteoglycans. *Exp. Eye Res.* 48:815–839.

van Adelsberg, J., J.C. Edwards, J. Takito, B. Kiss, and Q. Al-Awqati. 1994. An induced extracellular matrix protein reverses the polarity of band 3 in intercalated epithelial cells. *Cell.* 76:1053–1061.

Wigler, M., S. Silverstein, L.S. Lee, A. Pellicer, Y.C. Cheng, and R. Axel. 1977. Transfer of purified herpes virus thymidine kinase gene to cultured mouse cells. *Cell.* 11:223–232.

Yeaman, C., A.H. Le Gall, A.N. Baldwin, L. Monlauzeur, A. Le Bivic, and E. Rodriguez-Boulan. 1997. The *O*-glycosylated "stalk" domain is required for polarized sorting of an apical membrane protein in MDCK cells. *J. Cell Biol.* 139:929–940.

Yoon, S.O., C. Lois, M. Alvarez, A. Alvarez-Buylla, E. Falck-Pedersen, and M.V. Chao. 1996. Adenovirus-mediated gene delivery into neuronal precursors of the adult mouse brain. *Proc. Natl. Acad. Sci. USA.* 93:11974–11979.

Yoshimori, T., P. Keller, M.G. Roth, and K. Simons. 1996. Different biosynthetic transport routes to the plasma membrane in BHK and CHO cells. *J. Cell Biol.* 133:247–256.

Zhao, S., L.J. Rizzolo, and C.J. Barnstable. 1997. Differentiation and transdifferentiation of the retinal pigment epithelium. *Int. Rev. Cytol.* 171:225–266.

Zinn, K.M., and M.F. Marmor. 1979. The Retinal Pigment Epithelium. Harvard University Press, Cambridge.

Zurzolo, C., A. Le Bivic, A. Quaroni, L. Nitsch, and E. Rodriguez-Boulan. 1992. Modulation of transcytotic and direct targeting pathways in a polarized thyroid cell line. *EMBO (Eur. Mol. Biol. Organ.) J.* 11:2337–2344.

Zurzolo, C., M.P. Lisanti, I.W. Caras, L. Nitsch, and E. Rodriguez-Boulan. 1993. Glycosylphosphatidylinositol-anchored proteins are preferentially targeted to the basolateral surface in Fischer Rat Thyroid epithelial cells. *J. Cell Biol.* 121:1031–1039.